CZESLAW KOZIARSKI[*)]

FRICTION COUPLING OF ROLLING ELEMENTS

In the paper, a new model of friction coupling in rolling friction is presented. Apart from slips related to elastic and plastic deformation in the area of actual contact of two bodies, the mechanism includes also inertia forces related to tangential deformations.

Research concerning a model of coupling mechanism of variable ratio friction wheels is described. The main objective of the investigation was to prove that the force acting along the contact line of friction wheels is significantly affected by the shape of the contact area which had not been taken into account in the relations applied so far. A new model of the coupling mechanism was suggested and verified experimentally.

List of important symbols

a	half length of the contact area between rolling elements,
A	adhesive tacking area,
α'	dimensionless coefficient of track deformability,
$\alpha_{1,2}$	half contact angle of a rolling element,
b	half width of the contact area between rolling elements,
c	deviation of the rolling point C,
Δh	misalignment of axes of rolling elements,
$\Delta_{1,2}$	distance between the tip of a rolling element and the contact line,
Δt	time for a rolling element to travel an assumed elementary contact area,
Δv	difference of displacements,
Δx	half dimension of the assumed elementary contact area,
E	substitute modulus of elasticity of friction wheel track,
$E_{1,2}$	modulus of elasticity of rolling element track,

[*)] *Wrocław University of Technology, Institute of Machine Design and Operation; ul. Łukasiewicza 7, 50-371 Wrocław, Poland; E-mail: koziarski@nwikem.ikem.pwr.wroc.pl*

f coefficient of rolling friction,

F friction force,

F_N pressure force of rolling elements,

F_S frictional interlocking force,

F_T peripheral force,

F_v longitudinal force (component of coupling force perpendicular to peripheral force),

F_x coupling force component perpendicular to the contact line,

F_y coupling force component parallel to the contact line,

$g_{1,2}$ track material density,

$G_{1,2}$ shear modulus of the track material,

l distance between the rolling point and the centre of the contact area,

l_N radius of action of friction coupling force,

μ coefficient of friction,

μ_0 coefficient of friction during close-to-zero slip,

$v_{1,2}$ Poisson's ratio,

v_{Mo} dimensionless coefficient of friction moment,

v_0 dimensionless coefficient of energy loss in the contact area of rolling elements,

v_y friction force capacity factor in the direction of the contact line of rolling elements,

v_T friction force capacity factor in the direction perpendicular to the contact line of rolling elements,

Ψ total to elastic deformation ratio,

p pressure,

p_0 maximum pressure,

r curvature radius of a rolling element in the contact area,

r' curvature radius of a rolling element generatrix in the centre of the contact area,

r'' curvature radius of a rolling element in the centre of the contact area,

r_z substitute curvature radius of a rolling element,

r_z' substitute curvature radius of a rolling element generatrix,

$R_{1,2}$ rolling element generatrix,

R_z substitute rolling element generatrix,

S contact area of rolling elements,

σ misalignment angle of the axes of rolling elements,

v peripheral velocity,

v_{el} elastic slip velocity due to the elementary friction force,

v_0 deformation slip velocity due to the elementary friction force,

$v_{x,y}$ components of geometric slip velocity in the centre of the contact area,

v_y relative velocity of rolling elements along the y axis coinciding with their contact line,

v_s slip velocity,

v_ω geometric slip velocity,

$T_{1,2}$ moment acting on a rolling element,

T_{Mo} friction moment (moment of sliding friction around the rolling point); in specific case - moment of pivoting friction,

$u(x,y)$ displacement components in the contact plane of rolling elements,

u_b computational vector sum of displacements of adjacent elementary contact areas on rolling elements,

$\omega_{1,2}$ angular velocity of a rolling element,

ω_0 angular velocity of pivoting friction.

1. Introduction

The process of friction has been long utilized in such mechanisms as friction transmissions and train brakes. Frictional contact is also a necessary condition for rolling motion to occur. In order to determine the magnitude and direction of the frictional interlocking force, it is necessary to know in advance these values for elementary friction forces acting at the interface. To establish these forces, it is necessary to determine velocities and directions of slipping at central points of elementary contact areas. The act of slipping is made up of a component called geometrical slip and another one resulting from deformational displacement along a plane where the central points of contact areas meet. Geometric slip is caused by relative motion between two bodies in contact. This motion is also considered to be the principal cause of deformational displacements.

2. Model of coupling

2.1. Coupling of surface rigid elements

Distribution of forces and slips in the contact area of rolling elements, resulting from the difference of their angular velocities in the contact area, is shown in Fig. 1. That difference, called velocity of pivoting friction, is:

$$\omega_0 = \omega_1 \sin\alpha_1 - \omega_1 \sin\alpha_2 , \qquad (1)$$

where: $\omega_{1,2}$ = angular velocity of a rolling element,

$\alpha_{1,2}$ = half contact angle of a rolling element.

Location of the rolling point C on the x axis is determined by the value c named deviation of rolling point, which causes the force F_y acting along the y axis:

$$c = v_y / \omega_0 . \qquad (2)$$

The component of slip velocity at the central point of the contact area, acting along the contact line of friction wheels, is:

$$v_y = v_v + f\omega_0 + v\sin\sigma , \qquad (3)$$

where:

v_v = relative velocity of the rolling elements along the y axis coinciding with their contact line,

f = coefficient of rolling friction,

v = peripheral speed,

σ = misalignment angle of the axes of the rolling elements.

Fig. 1. Mechanism of planar frictional contact between rolling elements

Location of the rolling point C on the y axis is given by the value l called its fairness. The v_x velocity component of geometrical slip at the central point of the contact area results from friction which conveys the force F_x, perpendicular to the contact line. The F_x and F_y forces constitute the frictional interlocking force F_S. Product of this force and its arm l_N makes the pivoting friction moment.

2.2. Coupling of flexible elements

The simplest method of determination of component coupling forces of a road wheel with its track is the linear Kalker's theory. This theory is deducted from de Platers' concept (1958), postulating that, when the geometric slip velocity is low enough, it is reduced down to zero in the whole contact area and

thus, energy losses caused by slip are eliminated [1]. The component forces of friction coupling are:

$$F_x = -abG_{1.2}C_{11}v_x, \qquad F_y = -abG_{1.2}\left(C_{22}v_y + \sqrt{ab}C_{23}\omega_0\right), \qquad (4)$$

where (see Fig.1 and 2):

$G_{1.2}$ = shear modulus of track material,

C_{11}, C_{22}, C_{23} = coefficients dependent on Poisson's ratio and the b/a ratio defining shape of elliptical contact area.

Therefore, these component forces are linear functions of velocity components v_x and v_y of geometrical slip in the centre of the contact area, called rigid slip, but they do not depend on each other. Besides, velocity of pivoting friction affects only the component force F_x of friction coupling, perpendicular to the rolling direction. Application of this method is recommended only when velocity of geometric slip does not exceed $0.001v$, but even then the results of calculations not always match the experiments. In other cases, Kalker recommends using methods considering the presence of slip in the contact area between wheel and track. Some of these methods, called non-stationary ones, taking into account not only elastic slip but also its time variability, are described in [1]. In these papers, beside some methods developed by other authors, Kalker presents his method named the exact one. In this method, it is assumed that component slip velocities in a point of the contact area are:

$$v_s(x, y) = (v_{\omega x} + \omega_0 y, v_{\omega y} + \omega_0 x) + u'(x, y, t) =$$
$$= (v_{\omega x} + \omega_o y, v_{\omega y} + \omega_0 x) + u'(x, y, t) - v(\partial u / dx) + (\partial u / dx), \qquad (5)$$

where:

$u = u_w - u_r$ = difference of displacements between wheel and track,

$v_{\omega x}$ and $v_{\omega y}$ = components of geometric slip,

t = time,

$\partial u/\partial t = 0$ = velocity of displacement (zero for a stationary process).

According to Love, the component elastic displacements are:

$$u(x, y) = \frac{1}{\pi G} \int_s \left\{ \left(\frac{1-v}{R} + \frac{v(x-x^*)^2}{R^3}, \frac{v(x-x^*)(y-y^*)}{R^3} \right) dF_x(x^*, y^*) + \right.$$
$$\left. + \left(\frac{v(x-x^*)^2}{R^3}, \frac{1-v}{R} + \frac{v(y-y^*)^2}{R^3} \right) dF_y(x^*, y^*) \right\} dxdy \qquad (6)$$

where:

$R = \sqrt{(x-x^*)^2 + (y-y^*)^2}$ = distance between the considered point in the contact area and the point of application of the elementary friction force dF of components dF_x and dF_y,

x^* and y^* = coordinates of the point of application of the elementary friction force in peripheral and perpendicular directions, respectively.

By contrast to other investigators (e.g. Kalker [1]) who determine the magnitudes and directions of slip at the wheel/track interface seeking minimum value of a potential function, the author has found these values for wheels in frictional contact assuming that the slip velocity is reduced by the elastic slip component due to the elementary friction force [2]. Application of this principle brings about various benefits, for example an easy explanation of surface inertia forces present within the deformed layer of the wheels due to elastic shearing deformation of the contact plane [3].

Fig. 2. Mechanism of frictional interlocking at contact point of rolling elements

In order to determine the arrangement of forces and slipping movements at the contact area of rolling elements, it was assumed that geometrical slip velocity v_ω due to pivoting friction (see Fig. 2), defined as:

$$v_\omega = \rho \omega_0 ,$$ (7)

where: ρ = position vector,
is added to slip velocity resulting from the difference of displacements caused by all the forces acting at the point in question. These displacements are not caused by the elementary friction force applied to it. The magnitude of the slip velocity vector is:

$$v_b = \frac{du_b}{dt} = v\frac{du_b}{dx} = v\left(\frac{\partial u_{bx}}{\partial x} + \frac{\partial u_{by}}{\partial x} \right),$$ (8)

where:

$$du_b = du_{b1}(x^*,y^*) + du_{b2}(x^*,y^*)$$ (9)

is vector sum of differentials of displacements accomplished by centres of adjacent elementary contact areas on the wheels 1 and 2.
The latter differentials are:

$$du_{b1,2}(x^*, y^*) = du'_{b1,2}(x^*, y^*) - du_{b1,2}(x^* -dx, y^*),$$ (10)

where:

$u'_{b1,2}(x^*, y^*)$ = surface displacement of the centre of the considered elementary contact area caused by all forces except dF applied in it,

$u_{b1,2}(x^*, y^*)$ = real surface displacement of the centre of the considered elementary contact area.

The sum of geometrical v_ω and elastic v_b components of slip velocity determines the direction of the elementary friction force and the corresponding elastic slip velocity. This sum is reduced by slip velocity due to the elementary friction force:

$$v_0 = -du_0 / dt = -vdu_0 / dx,$$ (11)

where:

$$du_0 = du_{01}(x^*, y^*) + du_{02}(x^*, y^*)$$ (12)

is the sum of displacements of the central points of the elementary contact areas, caused by this force.
Real value of slip velocity is:

$$v_s = v_v + v_b - v_0.$$ (13)

When the obtained result is negative, it is assumed that there is non-developed friction, so v_s equals to zero and the elementary friction force is:

$$dF = p\mu \frac{v_v + v_b}{v_0} dS .$$ (14)

Since there was no need of defining and performing iterative steps, application of the described method in numerical calculations of forces and slips in the contact area of friction wheels significantly reduced the calculation time. This enabled the author to undertake a trial to consider inertia forces in surface layers of rolling elastic bodies.

In Figure 2, the elementary inertia forces connected with elementary masses of the deformed active surface layer of the friction wheels, named surface forces, are designated as dF_b:

$$dF_{b1,2} = g_{1,2} \frac{d^2 u_{1,2}(x^*, y^*)}{dt^2} dxdydz ,$$ (15)

where:

$g_{1,2}$ = material density of active surface of the rolling element.

When applying the finite element method, it can be assumed according to (11), that slip velocity caused by the elementary friction force is:

$$v_0 = \frac{\Delta u_{01} + \Delta u_{02}}{\Delta t},$$ (16)

where:

$\Delta u_{01,2}$ = tangential displacement caused by the elementary friction force,

$$\Delta t = 2\frac{\Delta x}{v}, \tag{17}$$

Δx = half distance of the centres of adjacent elementary contact areas.

Assuming for simplification that one of the friction wheels is surface rigid, the elementary contact area is a square of side $2\Delta x$ loaded by the elementary force dF with uniform tangential stress p_u acting along the x axis, the Love's formula (14) takes the simplified form:

$$\Delta u_{el} = \frac{pm}{pG_{1.2}} \int_{-Dx}^{Dx} \int_{-Dx}^{Dx} \frac{x^2 + (1-v_{1.2})y^2}{\sqrt{(x^2 + y^2)^3}} dxdy, \tag{18}$$

and, after integration:

$$\Delta u_{el} = \frac{4p\mu(2-v_{1.2})\Delta x}{\pi G_{1.2}} \arcsin h1, \tag{19}$$

where:

μ = coefficient of friction,
$v_{1.2}$ = Poisson's ratio,
$G_{1.2}$ = shear modulus of track material.

Dividing the above expression by Δt one obtains elastic slip velocity caused by the elementary friction force:

$$v_{el} = \frac{4p\mu(2-v_{1.2})v}{\pi G_{1.2}}, \tag{20}$$

The above formula and the finite difference method were used to derive the following relationship for elastic slip velocity of a particular rolling element, caused by the assumed elementary friction force.

The elastic slip velocity is independent on size of the assumed elementary contact area, i.e. of increments of numerical quadrates. Thus, it is possible to accept the formula (20) as valid also for the point contact. This served as a lemma to prove validity of the accepted principle, called here the kinematic law of friction [4], [5].

Assuming the formerly recommended by Niemann values of friction coefficient and permissible pressure in calculations of coupling of dry running friction wheels, it is possible to determine the following maximum speed velocities caused by the elementary friction force:

$v_{el,max} = 0.018476v$ for textolite by steel
(when $p_0 = 149$ MPa, $\mu = 0,4$, $v = 0.3$ and $E = 8000$ MPa),

$v_{el,max} = 0.3222v$ for gum by steel
(when $p_0 = 6.38$ MPa, $\mu = 0.8$, $v = 0.5$ and $E = 40$ MPa).

The above values were calculated disregarding deformation of the steel wheel.

In the case of steel by steel, considering deformation of both collaborating elements and accepting $p_0 = 3936$ MPa, $\mu = 0.2$, $v = 0.3$ and $E = 2.1 \cdot 10^6$ MPa, the maximum speed velocity is:

$$v_{el,max} = 0.018593v.$$

The obtained results prove possible significant influence of elastic slip caused by the elementary friction force on the elastic slip velocity in the contact point of rolling friction elements. In many cases, this component can exceed the geometric slip velocity and it is known not to be the only component of slip velocity due to the elementary friction force.

In Figure 3, calculation results of relative values of longitudinal forces v_v obtained using Kalker's programs are compared with those obtained using a newly developed program called PUNKT with the presented method. The diagrams are drawn as functions of dimensionless deformability coefficient of tracks of the rolling elements, being inverse coefficient Ψ (see Figure 3) used by Kalker:

$$\alpha'' = 40\mu\rho_0 v/(aE\omega_0), \tag{21}$$

where E is substitute elastic modulus of track material:

$$E = \frac{2E_1'E_2'}{E_1' + E_2'}, \tag{22}$$

$$E_{1.2}' = \frac{E_{1.2}'}{1 + v_{1.2}^2}. \tag{23}$$
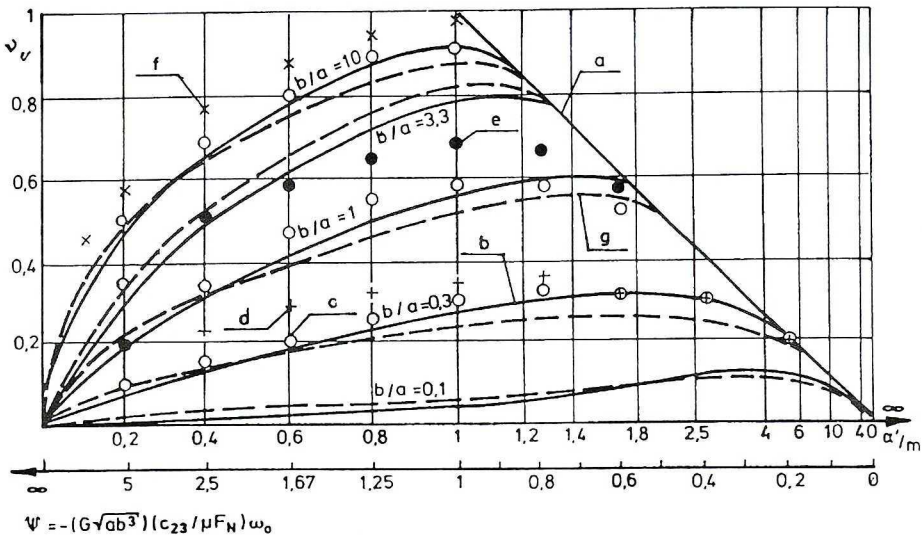
Fig. 3. Comparison of computational values v_v obtained with PUNKT program and those obtained with Kalker program at $c = l = 0$. Designations: a - linear theory, b - CONTACT, c - DUWOROL, d - FASTSIM ($b/a = 0.3$), e - FASTSIM ($b/a = 1$), f - FASTSIM ($b/a = 10$), g – PUNKT

The results obtained using the CONTACT program are marked with heavy lines and those obtained with the PUNKT program - with broken lines. The factor of proportionality m is different for individual values of b/a. It is chosen to maintain conformity of the calculated values with the linear Kalker's theory in the range of large values of α'. The programs CONTACT and PUNKT were developed on the ground of the exact method and the program FASTSIM - on the ground of the approximate method which, on the expense of accuracy, significantly reduces the calculation time.

Velocity v_0 is larger than that calculated from the formula (5) since there is plastic deformation and elastic shearing deformation within the contact area. It is the actual contact area where surface cracks are observed to originate and frequently end up in severe surface damage. There is no method available to calculate these deformations - the approach presented in [7], works only for a model of two elements touching each other, and only plastic deformation is taken into account. It is clear from the analysis provided in [7] that displacements within the actual contact areas may be much larger than those resulting from the elastic semi-three-dimensional model. Further confirmation of this fact was offered by experimental investigations on slip friction [8]. Referring once more to Fig. 2, slip velocity due to deformations other than the elastic ones and associated with the elementary friction force is denoted by v_{sb}.

Plots in Figures 4, 5 and 6 show basic characteristics of the interlocking process between two wheels with rubber lining as functions of dimensionless coefficient of deformability of the active area α'.
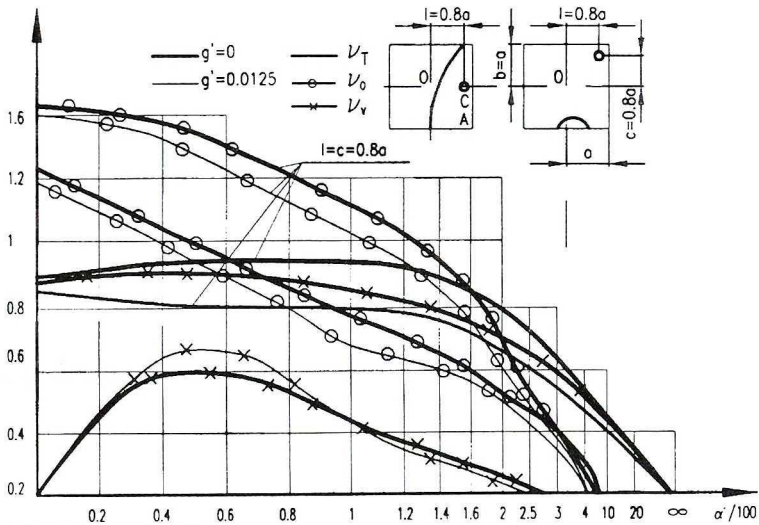
Fig. 4. Effect of deformational slip on basic characteristics of interlocking between rolling elements for linear contact at $b/c = 1$; a) - both elastic deformation and surface inertia forces considered, b) - additional elastic-plastic deformation and twofold increase of static friction coefficient as compared with the kinetic coefficient considered, c - as in a) and b)
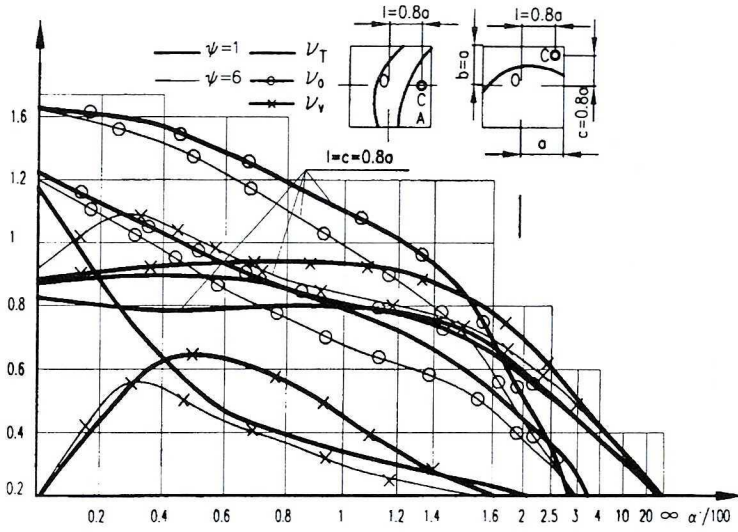
Fig. 5. Effect of deformational slip on fundamental coupling parameters
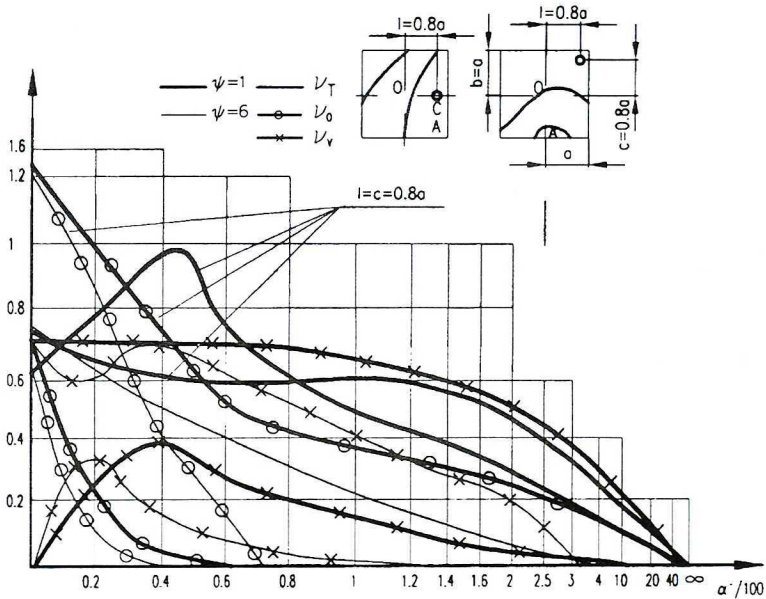for point contact at $b/a = 1$

Fig. 6. Effect of deformational slip on fundamental coupling parameters for point contact, the
difference of friction coefficients considered at $b/a = 1$

The characteristics were calculated for two different values of the dimensionless
index of track material density:

$$g'_{1,2} = \mu g_{1,2} v^2 / (4\pi G_{1,2}),$$ (24)

where $g_{1,2}$ is track material density for two different values of the total to elastic
deformation ratio Ψ:

$$\Psi = v_0 / v_{el},$$ (25)

and for two different values of the coefficient of friction.

It is clear from the plots that the elastic slip has considerable effect on
characteristics of frictional contact between two wheels. This is the reason why
the decrease of power due to energy P_t lost in slip intensifies with increasing
coefficient α':

$$v_0 = P_t / (\mu a F_N \omega_0).$$ (26)

Relative values of the peripheral force

$$v_T = F_x / (\mu F_N),$$ (27)

rise somewhat at the beginning and then decrease to zero. Relative values of the
longitudinal force

$$v_v = F_y / (\mu F_N),$$ (28)

vary in similar way, but it is to be noted that for $c = 0$ they rise starting from
zero to reach considerable levels and then again decrease to zero. Elastic-plastic
deformations act similarly as surface inertia forces, i.e. their effect on the
dimensionless index of the lost energy power is stronger than on the v_T and v_v
values or, in other words, on the frictional interlocking force F_S.
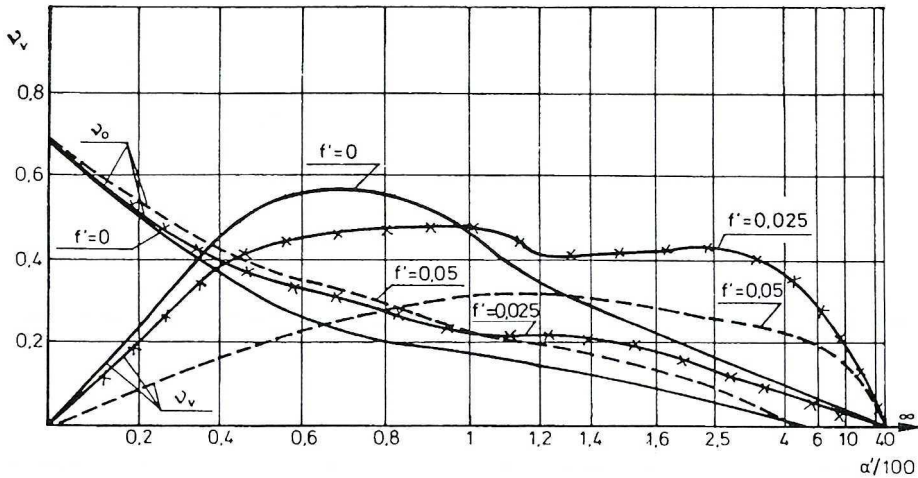
Fig. 7. Effect of elastic slip on basic parameters of friction wheels coupling for point contact, large
share of inertial forces at $b/a = 1$ and $c = l = 0$

The above is confirmed also by the results obtained using the PUNKT program, calculated for much larger values v_v and presented in Figure 7. Besides, it is visible that the surface inertia forces considerably rise the longitudinal force for large α' values.

In right-hand top corners of the diagrams in Figures 4, 5 and 6, the contact areas with various positions of the rolling point C are shown. Depicted are particular interlocking areas from the point C due to elastic slip. The areas denoted by A, found for $\alpha' = 101$, become larger with rising value of the coefficient. They also increase considerably when the surface inertia forces, plastic deformation and difference in friction coefficients are taken into account.

The kinematic law of friction has been effectively employed to the analysis of the friction wheel coupling mechanism. It proved that the analyses of the tyre-rigid ground coupling mechanism (detailed calculation in [4] and [5]) and of the rim-rail contact phenomena ([9] - among others) are equally useful.

3. Investigation of coupling of rolling elements

3.1. Investigation of coupling of rolling elements at high velocity pivoting friction

Ratio of friction coupling distribution is dependent mainly on the distribution of contact force and on relative values of rolling point co-ordinates l/a and c/a, as was presented in [13]. The desired contact force distribution can be obtained by proper choice of geometry and material of friction wheels and of the value of the contact force itself. Linear contact was applied in order to obtain possibly highest stability of pressures during the measurements and thus - the highest repeatability of measurement results. To the very end, the ratio b/a was assumed equal to 1 and 2, for which practical limiting values of the ratio of contact surface dimensions yielded maximum efficiency. Lining of the wheel 2 with more active surface (the driven wheel, in this case) was made of textile laminate, the material most commonly applied, and running-in period was fairly short. The driving wheel was made of Polish steel grade 45. To obtain the most stable elastic properties, the lining was made so that principal stresses were perpendicular to fabric layers.

At the same time, this ensured the coefficient of friction not too much dependent on the direction of slip velocity. Application of textile laminate resulted in fairly large dimensions of contact area despite small radii of the friction wheel surfaces. This allowed for determination of the dimensions of that area with sufficient accuracy. To be even more exact, rotation axes of friction wheels were situated on the opposite sides of the contact area. This made it possible to measure the average transmission ratios in relatively short time, with negligibly small calculation error of rolling point distance.

The main objective of the experiments was to prove that the value of the coupling force component F_y was affected by the ratio of the dimensions of the

contact area. To obtain sufficiently accurate force measurements, the bearings of the passive wheel 2 were mounted in the yoke 3 that, in turn, could swing around the axle 4 (see Fig. 8 and 9).
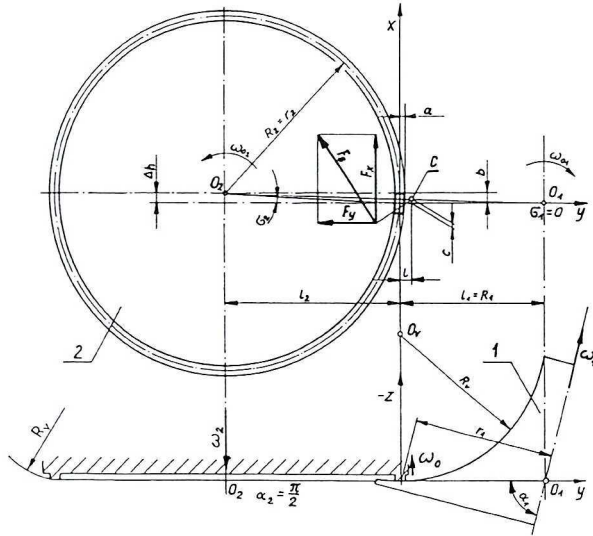

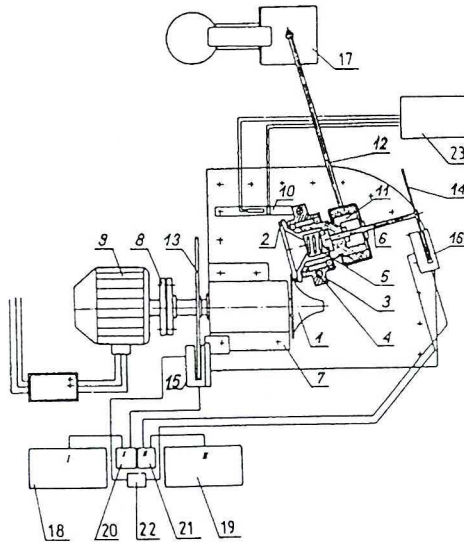Fig. 8. Lay-out of coupling model of friction wheels under investigation

Fig. 9. Lay-out of testing stand: 1 - active friction wheel made of steel, 2 - passive friction wheel with textile laminate lining, 3 - driven wheel yoke, 4 - axle of yoke, 5 - friction wheel pressing spring, 6 - spring pressure adjusting screw, 7 - active wheel bearings, 8 - flexible coupling, 9 - driving motor, 10 - strain gauge dynamometer, 11 - brake drum, 12 - brake, 13 and 14 - stroboscope discs, 15 and 16 - photoelectric cells with lamps, 17 - dynamometer, 18 and 19 - electronic counters, 20 and 21 - photoelectric pulse amplifiers, 22 - special switching-off device (timer), 23 - strain gauge bridge

Consequently, the bearings of the generatrix of the driving wheel 1 had to be of circular shape with curvature radius R_v of 42.5 mm. Influence of the longitudinal forces F_v on the effective pressing force was avoided by making the shape of active surface on driven wheel lining very close to a flat disc. The driven wheel was pressed axially against the driving wheel. Outside and inside diameters of active surface of the lining were 104.4 mm and 97.6 mm, respectively. Axial pressing force F_N equal to 96.2 and 385 N was exerted by a spring of variable tension. Pressure direction and shape of the lining of the wheel 2 ensured practical invariability of its active surface dimensions independent on wear.

3.1.1. Method of investigation

Since accurate values of friction coefficient were unknown, and determination of the effect of slip direction and - first of all - of rolling point location on the value of friction coefficient were impossible, it was necessary to carry out measurements of both the forces F_v and the rolling point distance. This could be done indirectly by measurements of actual transmission ratio. Measurements of F_v were performed using a strain gauge dynamometer 10. Due to its application, position of the wheel 2 was kept practically constant. Calibration of the dynamometer was carried out using weights with accuracy of 0.098 N. This corresponded to force measurement accuracy of the order of $(102/42.2) \times 0.098 = 0.235$ N. Deviation resulting in longitudinal forces could be obtained only by shifting the axes out of co-planar position. This was practically done by changing the location of the driven wheel yoke along its swinging axis by the distances of $h = 0$ and $h = 1.06$ mm, resulting in relative deviation of the rolling point $c/a = 0$, 0.4 and 1 (at $l = 0$). To bring working conditions of the model closer to those existing in actual structures, location of the rolling point was changed by changing the driven wheel moment using a shore brake with mechanical feedback. Application of the brake resulted in automatic stabilization of the value of loading moment T_2.

Measurements of moment were carried out using a tangent balance of the accuracy of 0.049 N, corresponding to accuracy of moment measurement of 0.0196 Nm. Transmission ratio was measured using light impulses produced by lamps and stroboscope discs 13 and 14. Light impulses were collected by photocells 15 and 16 and counted by electronic counters. The same counting time was ensured by appropriate coupling of switches. In this way, an arbitrarily high accuracy could be obtained provided that measurement time was sufficiently long.

Measurements of transmission ratio were carried out at rotational speed of the driven wheel 12 equal to 240 rpm what corresponded to peripheral speed of 1.03 m/s. Such a low value of peripheral speed was chosen in view of relatively high value of $\omega_0/\omega_l = 1.77$ which resulted in pivoting friction velocity of the other wheel of $\omega_0 = 44$ rad/s and in view of the fact that thermal resistance of textile laminate was not very high.

3.1.2. Measurement results and conclusions

Since the peripheral velocities of both wheels are identical at the rolling point C, it can be written that

$$1 = \frac{\omega_{01}l_1 - \omega_{02}l_2}{\omega_{01} + \omega_{02}}, \tag{29}$$

where (according to Fig. 2) $\omega_{01} = \omega_1 \cdot \sin\alpha_1$ and $\omega_{02} = \omega_2$. Considering the above and dividing both sides of (29) by half length a of the contact area, one obtains the relative distance of the rolling point as:

$$\frac{l}{a} = \frac{l_1 \sin a_1 + l_2 i_k}{a(\sin a_1 + i_k)}, \tag{30}$$

where $i_k = \omega_2/\omega_1$ is kinematic transmission ratio.

In a similar way, a formula for c can be derived:

$$c = \frac{\omega_{02}\Delta h}{\omega_{01} + \omega_{02}} = \frac{\Delta h i_k}{\sin\alpha_1 + i_k}. \tag{31}$$

When kinematic transmission ratio i_k is substituted by l from the formula (30), a relationship for relative deviation is obtained:

$$\frac{c}{a} = \frac{\Delta h(l_1 - l)}{a(l_1 - l_2)}. \tag{32}$$

The value of computational coefficient μ_v along the direction of longitudinal force F_v was calculated from the formula:

$$\mu_v = \frac{T_v}{F_N v_v R_v} = \frac{F_v}{F_v v_v}, \tag{33}$$

where:

T_v = yoke moment,
F_N = pressing force of friction wheels,
v_v = computational degree of friction force utilization along the direction of peripheral force.

Starting from the relationship

$$T_2 = F_x \left[l_2 + l - \frac{T_0}{F_x} \right] - F_y (\Delta h - c), \tag{34}$$

where T_0 is pivoting friction moment, computational friction coefficient μ_{Mo} of energy loss is equal to the coefficient μ_T along the direction of peripheral force. After some transformations of (34) it is obtained:

$$\mu_T = \frac{T_2 + F_N \mu_v (\Delta h - c)}{F_N (l_2 + l) v_T - a v_0}, \tag{35}$$

where v_T and v_0 are computational degrees of friction force utilization along the direction of peripheral force F_x and computational coefficient of losses,

respectively. Values of the above equation were roughly determined in [10], and more detailed analysis was presented in [11].

Figures 10 and 11 present the measured and computational values of forces F_y as computational coefficients μ_T and μ_v dependent on relative distance l/a for $b/a = 1$ and 2 obtained for pressing forces $F_N = 6.2$ N and 385 N. Besides, the values of moment T_2 on the passive wheel resulting in variations of distance l are also shown. Each of the discussed drawings concerns different value of relative deviation c/a. It can thus be concluded that longitudinal force F_y is significantly affected by the shape of the contact area represented by b/a ratio.
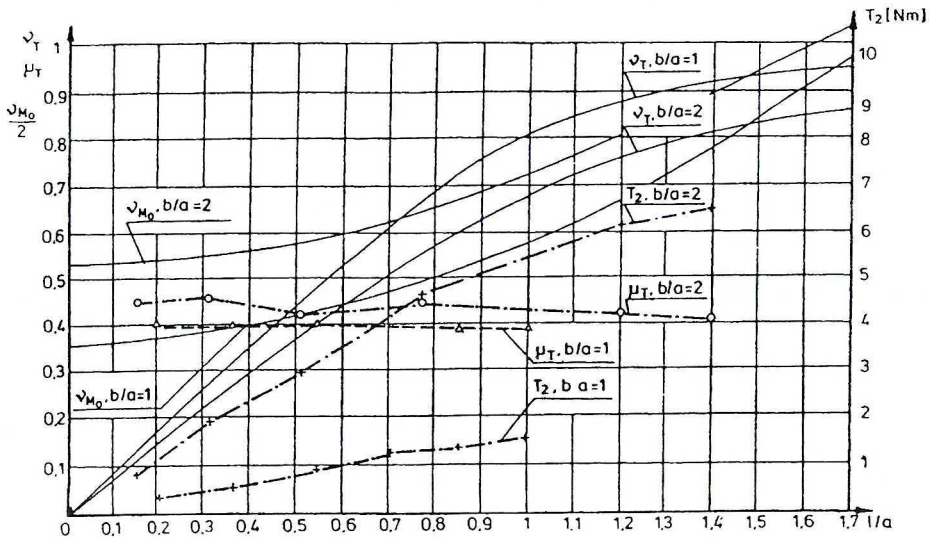
Fig. 10. Results of measurement of frictional coupling at $c = 0$
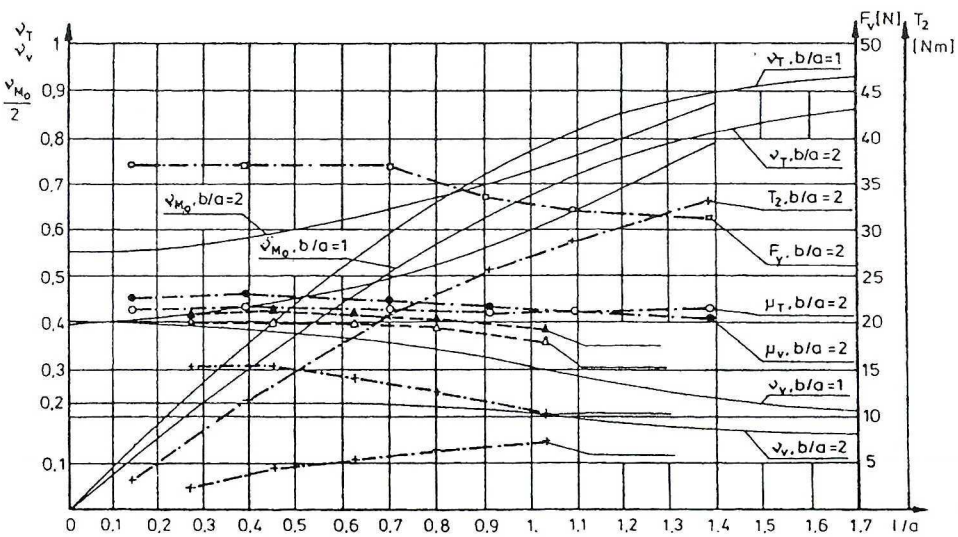
Fig. 11. Results of measurement of frictional coupling at $c/a = 0.4 - l/(87.7a)$

3.2. Investigation of coupling of rolling elements at medium velocity pivoting friction

3.2.1. Test stand

In order to obtain more complete verification of the presented in chapter 1 model of mechanism of coupling in rolling friction, investigation was carried out, among others, on suitably adapted test stand shown in Fig. 12 and Fig. 13. The stand consists of a disc wheel 1 pressed against cylindrical wheel with rubber friction lining 2. The wheel 1 is fitted on the end of vertical shaft 3 with its upper part seated in a bearing 4. Tensometrical dynamometers 5 fix the position of this bearing in horizontal plane with regard to the body 6 and are used for measurement of friction coupling component forces of the wheels. The four-articulated clutch 7, connecting opposite side of the bearing 4 with this body, prevents its rotation and allowes for displacement in all directions. A tensometrical momentometer 8 is used for measurement of torque transmitted to the shaft 3 through self-adjusting four-articulated clutch 9 from the reduction gear 11. The rings 10 connect the extensometers with a measurement bridge. The shaft 12 serves as an axis of rotation of fitted on it wheel 13 and movable body 14. The position of this body with regard to the body 6 where it is supported, is fixed with the screw 15 enabling adjustment of twist of axes of the friction wheels 1 and 2 and thus, adjustment of deviation of the rolling point C. The latter wheel is slidably fitted on the hollow shaft 16 supported on self-aligning bearings in the movable body 14.
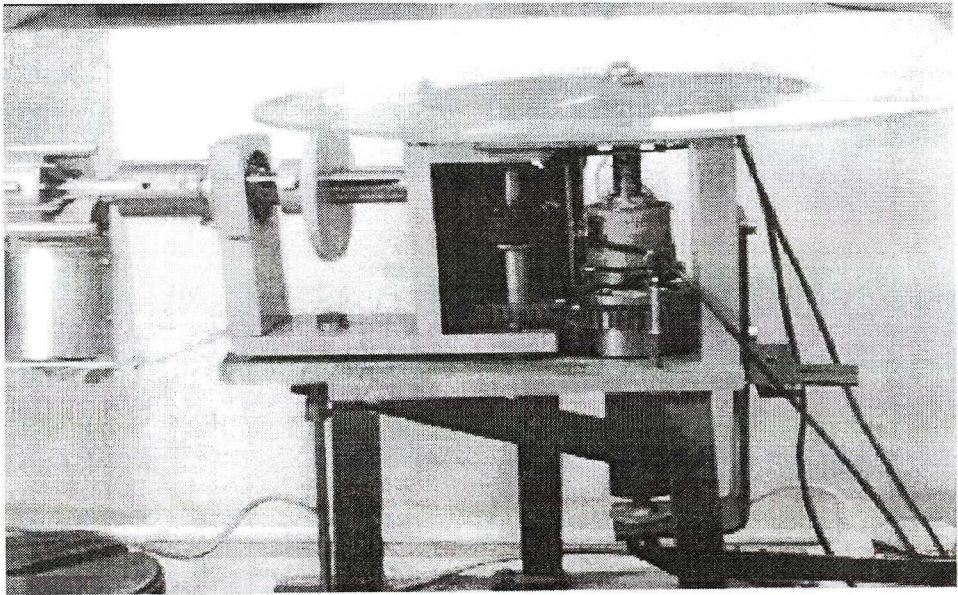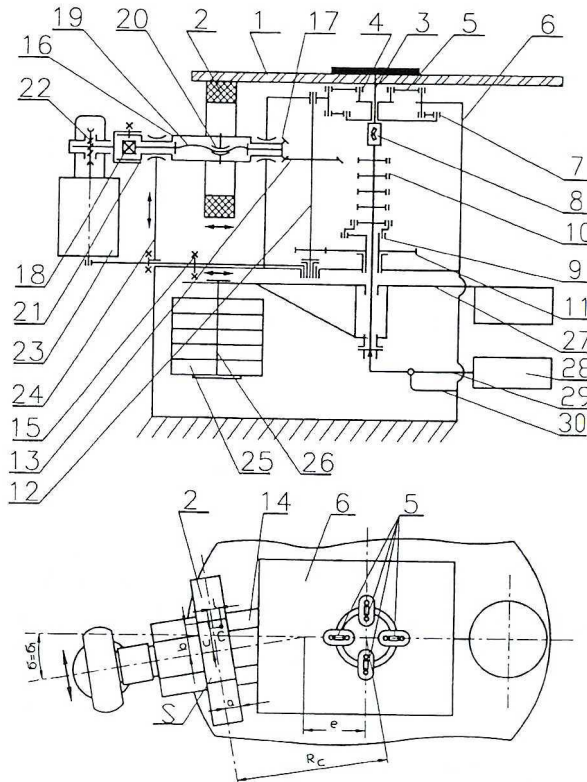

Fig. 12. View of test stand

Fig. 13. Lay-out of test stand

One end of this shaft is equipped the with tapered gear 17 co-operating with the wheel 13 and the other end with the handwheel 18 of the guide screw 19 that, with the nut 20, shifts the friction wheel 2 along its contact line with the wheel 1. Thanks to this, it is possible to adjust the distance l of the rolling point C from the centre of contact area O. The shaft 16 is driven by the electric motor 23 through the sleeve 21 connected with the worm gear 22. One end of this shaft is supported on the movable support 24, enabling compensation of deflection of the wheel 1. Pressure of the friction wheels is acquired with the weights 25 hanging on the sling 26 with possible movement of its axis along one end of the bracket 27. This allowes for coincidence of the axis with the centre of the contact area of the friction wheels. On the other end of the bracket 27 a counterweight is placed to balance the bracket and the sling 26 so that their centre of gravity coincides with the axis of the shaft 3 on which the bracket is hanged in rotary way. The counterweight 28 fitted on the lever 29 supported on the bracket 30 compensates gravity force of the system pressing the friction wheels.

Diameter of the friction wheel 2 with rubber lining used in the investigations was $d = 125$ mm and the track width was $2a = 8$ mm. Radius of the rolling wheel on the disc wheel 1 was $R_c = 166.3$ mm. Measurements of forces and moment were taken at the following positions of the centre of the contact area: $l = -20, -10, -3.2, 0, 3.2, 10, 20$ mm and $c = 0$ and 8 mm with regard to the position of the rolling point C, where

$$c = e \cdot \sin \sigma = 70.2 \sin \sigma \quad [\text{mm}].\tag{36}$$

3.2.2. Objective and course of investigations

The main objective of the investigations carried out on the presented test stand was to confirm that deformational slip in the contact point of rolling elements like friction wheels is larger than elastic slip. Since the stand was equipped also with the disc wheel 1 made of transparent organic glass, an orthogonal grid of co-ordinates was cut on its active surface. On the active surface of lining of the wheel 2, made of white-coloured rubber, a millimetre grid of co-ordinates was drawn enabling observation of deformation of the contact surface through the transparent wheel 1 and thus, observation of deformation of friction lining of the wheel 2 as well. Using the pressure force $F = 9, 21, 36$ and 144 N it was possible to obtain the values $b/a = 0.5, 0.75, 1, 2$, and change of working conditions of the transmission expressed by change of coefficient of deformability of the active area α' in calculated range from ca. 100 to ca. 1500. The measurements were taken in both directions of rotational speed of the friction wheel 2, being 24, 48 and 72 rpm. The measurement gauges were calibrated using special levers. Three measurement bridges were used, type AR 405C. The results were recorded by a signal recorder MC 201A on hard disc of a microcomputer. The contact area was observed using a camera type CCD, model 1/3"-B/B, and the images were recorded with a video recorder on magnetic tape and with graphic card Video Blaster SE100 on the computer disc. The results recorded on individual frmes were compared with each other, so it was possible to discover any slip appearing between the friction wheels in their contact point. Then, the stand was modernized so that instead of swinging drive, a continuous drive of three different speeds was used. To compensate deflection of the disc wheel 1, the hollow shaft 16 was supported on self-aligning bearings enabling changes of its angle not only in horizontal but in vertical plane as well.

3.2.3. Measurement results and conclusions

In Figures 14 and 15, the measurement results of components of friction coupling forces and of torque moments are presented, obtained for different positions of the rolling point and for different pressure forces. Although the experiments were carried out at three different speeds, the results for one speed only are presented.
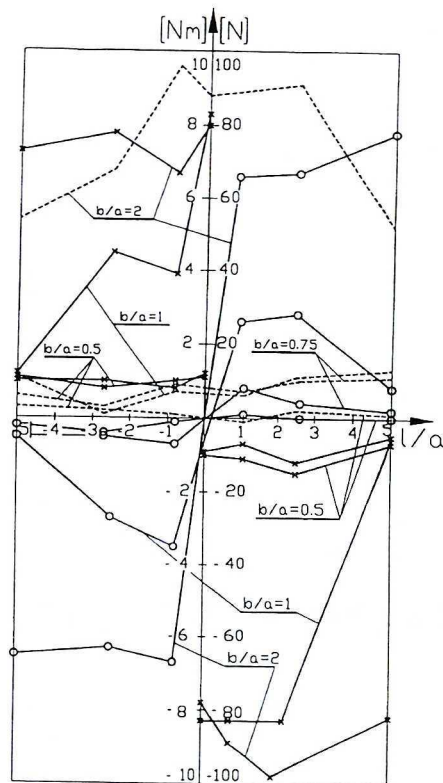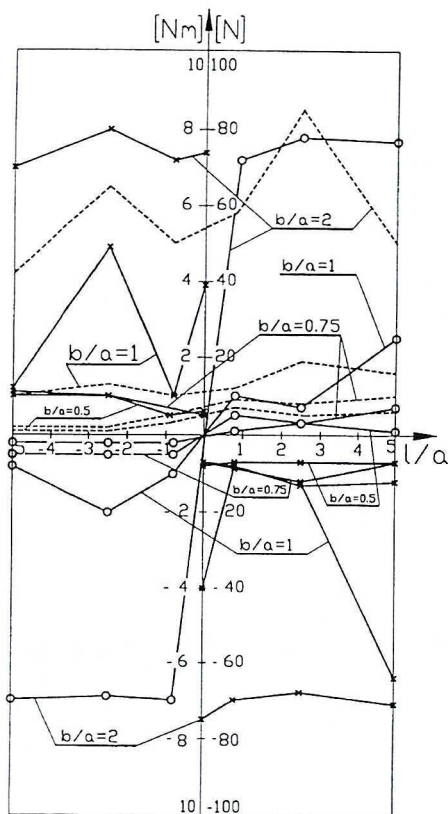
Fig. 14. Results of measurements of forces
and moment at $c = 0$:
x-----x moment T_{Mo}
o-----o peripheral force F_T
-------- longitudinal force F_v

Fig. 15. Results of measurements of forces and
moment at $c/a = -2$; lines as in Fig. 14

The reason is that even if for many measurements the results were substantially different, the differences were incidental. First of all, in these figures it can be seen that the values of peripheral forces not always increase under the influence of pressure force.

Comparison of the results obtained for different pressure forces and therefore for different values of α' proves unexpectedly stronger effect of elastic slip on parameters of friction transmission. This confirms the statement that velocity of slip which reduces geometric slip may be higher than velocity of elastic slip due to the elementary friction force and, for the same reason, the effect of pressure force may be stronger. The values of forces and moments in the contact plane of the friction wheels increase much more slowly with pressure force of the wheels than it would arise from elastic deformations. At some positions of the rolling point, insensitivity of the transmission for changes of pressure force appeared. This means that no significant changes of peripheral force were observed, and

that no significant changes of components of coupling force and measured moment were observed despite multiple changes of pressure force at fixed transmission ratio. However, their value increased much faster with increasing distance of rolling point from the centre of the contact area. This evidences the existence of higher slip velocity $v_{\varepsilon\lambda}$ due to elementary friction force than that resulting from elastic deformation. The above was confirmed also by observations of changes of deformation of the contact area, carried out on individual film frames of the recorded measurement results. Comparison of the frames revealed that the contact areas A are much larger than it results when elastic slips only are considered.

4. Conclusions

As it results from the presented considerations, the coupling mechanism in rolling friction is much more complicated than it is commonly thought. Even the influence alone of surface inertia forces on parameters of friction coupling may by very significant. These forces can appear not only as a result of tangential deformation but of radial deformation as well. Even more effect on parameters of coupling can result from plastic deformation on actual contact surfaces, in connection with non-dilatational elastic deformation. Of the most importance is, yet, the value and distribution of pressure in the contact area of the rolling elements in connection with the value of coefficient of friction. Pressure depending on pressing force is a function of deformability and shape of active surfaces of the elements, which changes because of wear. So, it depends on many factors, in similar way as coefficient of friction depends mostly on temperature in the contact point and on condition of active surfaces of the rolling elements. The surface condition can result from temperature, e.g. in the case of seizing.

Complexity of the problem is also confirmed by the proceeding and the results of the experiments. The derived relationships indicate strongly non-linear process of the phenomena. In turn, this results in large scatter of the results of calculations and measurements. The total of the gained experience inclines the author to state that these problems should be considered as determined chaos, what was already underlined in [2].

REFERENCES

[1]   Kalker J.J.: Mathematical models of friction for contact problems in elasticity. Wear, 113 (1986), p. 61÷77.

[2]   Koziarski C.: The modelling of the friction process of friction wheels. 3rd International Tribology Congress EUROTRIB'81, Warszawa - WSI Radom 1981, vol. l/A, p. 227÷232.

[3]   Koziarski C.: The mechanism of friction wheels coupling. Effect of elastic slip on coupling parameters. EUROTRIB '89 – 5th International Congress on Tribology, Tampere Univ. Technol. Finland, Tech. Res. Cent. Finland, Norwegian Inst. Technol. Norway, Helsinki 1989, p. 151÷156.

[4]   Koziarski C.: A kinematic law of friction - the proof and possible applications, Proceedings of the Japan International Tribology Conference, Nagoya 1990, Japanese Society of Tribologists, vol. 4, p. 1473÷1478.

[5]   Koziarski C.: Das kinematische Gesetz der Reibung. Tribologie und Schmierungstechnik, 39, Nr. 5, p. 288÷293.

[6]   Koziarski C., Maciejewski K.: Model of interlocking contact in friction wheels (in Polish). XVII Symposium on Machine Design, Lublin - Nałęczów 1995, Poland, Proceedings - Part I, p. 474÷479.

[7]   Skalski K.: The Contact Problem for Plastic-Elastic Bodies (in Polish). Warszawa, WNT, 1986, p. 14.

[8]   Konowalski K.: Effect of non-linear normal and tangential flexibilities of the contact areas on strength and rigidity characteristics of machine tool guideways. Doctoral Thesis (in Polish). Szczecin Tech. Univ., Dept. of Machine Construction and Shipbuilding, 1983.

[9]   Koziarski C.: Connection of the wheel-rail (in Polish). XI Konferencja Naukowa Pojazdy Szynowe, Kraków i Szczawnica 1995, Proceedings - Part II, p. 98÷106.

[10]   Koziarski C.: Effect of the longitudinal slip on the friction wheel coupling mechanism. EUROTRIB '85 - 4th International Congress on Tribology, Ecully - France, Vol. 4. Sec. 5.1; Amsterdam: ELSEVIER 1985, p. 1÷5.

[11]   Koziarski C.: Coupling of friction wheels in variable-speed transmissions (in Polish). Prace Naukowe Instytutu Konstrukcji i Eksploatacji Maszyn Politechniki Wrocławskiej 73, Seria: Monografie 24, Wrocław 1993.

[12]   C. Koziarski, Effect of temperature changes on coupling mechanism in rolling friction (in Polish). XXI Jesienna Szkoła Tribologiczna, Łódź - Arturówek, 1996.

[13]   Koziarski C.: Investigation on friction wheels coupling mechanism. EUROTRIB'93 - 6th International Congress on Tribology, Budapest 1983, Hungarian Academy of Sciences Vol. 4.4, p. 424÷433.

Sprzężenie cierne elementów tocznych

Streszczenie

W artykule przedstawiono nowy model sprzężenia ciernego w tarciu tocznym. Oprócz poślizgów związanych z odkształceniem sprężystym i plastycznym na powierzchni rzeczywistego styku dwóch ciał, model uwzględnia również siły bezwładności wywołane odkształceniami stycznymi.

Opisano badania modelu sprzężenia w przekładni ciernej o zmiennym przełożeniu. Głównym celem tych badań było wykazanie, że na wartość siły działającej wzdłuż linii styku kół ciernych istotny wpływ ma kształt pola styku, którego nie uwzględniano w dotychczasowych modelach. Przedstawiony nowy model sprzężenia ciernego został zweryfikowany doświadczalnie.